A tensioned cable as an adaptive tuned vibration absorber for response suppression in rotorcraft

J. L. du Bois [1]**, N. Lieven** [1]**, S. Adhikari** [2]
[1] Department of Aerospace Engineering, University of Bristol,
Queen's Building, University Walk, Bristol BS8 1TR, UK
e-mail: Jon.duBois@Bristol.ac.uk

[2] College of Engineering, Swansea University,
Singleton Park, Swansea SA2 8PP, UK

Abstract

Vibration suppression is a key focus in rotorcraft development, where complex periodic aerodynamic loading results in high levels of forcing transmitted through the rotor hub. Reduction of the resultant fuselage response offers benefits in terms of performance and ride quality. While full size rotorcraft have typically employed fixed rotor speeds, newer configurations are increasingly exploring variable rotor frequencies as a means of expanding the flight envelope of the vehicles. It is in this context that active and adaptive vibration control techniques become not only advantageous but necessary. Active methods employ actuation to superimpose forces on the ambient excitation, and range from hydraulic rams attached to the gearbox to piezoelectric elements embedded in the rotor blades to augment the lift. Adaptive methods offer the advantage of significantly lower power requirements, taking advantage of passive vibration absorption devices with adaptable stiffness and damping properties. The tuned vibration absorber (TVA) is a passive device with a long history of success in the mitigation of vibrations; its use has been seen in rotorcraft, for example, in the highly successful bifilar vibration absorber designs. In general, TVAs perform very well under specific operating conditions but are less useful and may even worsen the response when the excitation frequency is outside the design envelope. This paper examines the use of a vibration absorber based on a taught cable, nominally stretched the length of a helicopter tail boom. The absorber can be tuned by changing the tension of the cable, responding to changes in the main rotor frequency. A novel aspect of this configuration lies in the distributed nature of the mass in the cable. This distributed mass produces a range of harmonic response frequencies, any of which may be used as the operational frequency of the device. An advantage offered by this effect is the ability to cover a wide range of frequencies using a small range of cable tensions. A disadvantage is the additional complexity and weight, and the prospect of adverse influence from the extra harmonics. This paper uses theoretical and experimental results to explore the behaviour of the device, highlighting the benefits and the shortcomings to be addressed.

1 Introduction

Tuned vibration absorbers (TVAs) have long been used for passive vibration control. Variously referred to as vibration neutralizers, dynamic vibration absorbers (DVAs), or undamped vibration absorbers (UDVAs), the devices provide a passive means of:

(a) creating an antiresonance at at specific location and frequency; and

(b) manipulating a natural frequency of a structure to avert coincidence with an excitation frequency.

Their mode of operation is described in detail in a plethora of textbooks, for example [1, 2, 3, 4]. They are useful in applications with a narrowband excitation frequency; rotorcraft are such an application, where the majority of the structural excitation is at the main rotor frequency and multiples thereof. This is caused by periodic variation of the aerodynamic blade loads in forward flight and the effects of trailing vortices from preceding blades. Mitigation of the resultant vibrations transmitted to the fuselage is a critical area of contemporary rotorcraft research. Reductions in fuselage response allow for lighter aircraft, improving range and efficiency. Component fatigue is reduced and maintenance schedules can be relaxed, improving safety and reducing operating costs. Intelligent vibration control allows aircraft to fly faster and with increased comfort for pilot and passengers. In new designs these features will help combine the advantages of a fixed-wing jet with the convenience of VTOL capabilities.

Unsurprisingly, the concept of TVAs has already seen some success in the context of helicopters, notably in the form of the bifilar absorber [5], which has the advantage of being adaptable to different excitation frequencies. As new designs for fast aircraft begin to employ variable rotor speeds to counter the problems of supersonic tip speeds, traditional passive vibration control becomes less effective and adaptive and active techniques must be explored. By including an adaptive element in a traditional TVA, the passive behaviour can be tuned on-the-fly to the operational conditions. This type of adaptive passive repsonse suppression has advantages over fully active systems in terms of low power usage and continued (albeit degraded) operation in the event of control system failure. Many implementations of adaptive TVAs (ATVAs) have been described in the literature, with the majority employing tunable stiffness elements. A comprehensive review was conducted by Sun *et al.* [6], and a more recent review can be found in [7].

In the current paper, a cable is employed as an ATVA, using the principle of stress stiffening to adapt the stiffness of the absorber through changes in cable tension [8, 9, 10]. The cable's deployment in a helicopter tail boom is investigated, where it can effect changes to the low order bending modes. This arrangement allows for straightforward and continuous tuning of the structural response.

Section 2 begins by describing the validation of a finite element (FE) model of a Lynx helicopter tail boom, and discusses features of the structure. The cable ATVA concept is developed in this context in Section 3. The design of a reduced-scale test structure is then outlined in Section 4, with representative vibration modes intended to mimic the Lynx tail boom. Baseline experimental results are compared with a numerical model and preliminary TVA demonstartions are presented. Conclusions are drawn in Section 5.

2   Lynx Helicopter Model

The Lynx Mk. 7 is pictured in figure 1, undergoing variability studies as part of a GARTEUR programme to improve modelling capabilities for predicting structural response [11]. The tests focused on the response of the tail boom, seen mounted on a reaction wall in Fig. 1(b). The work presented here uses data from these tests to validate a FE model of the tail boom, and this model is then used for the subsequent ATVA investigations.

The FE model was supplied by QinetiQ and imported to ANSYS [12], where the tail boom was isolated for comparison with the experimental data. The tailboom model consists of 2185 nodes, 3519 elements and 13 coupling/constraint equations. It is predominantly comprised of shell elements describing the fuselage shell and ribs, with beam elements representing stringers and key elements such as the 8c struts used to stiffen the fin. Point masses are included to represent gearboxes and tail rotor assemblies. The tail rotor was also approximated in the experimental results using an equivalent steel mass at the hub attachment.

The model is constrained at the tail root, mimicking the stiff mounting to the reaction wall. The modal response of the model is compared with the experimental results in Fig. 2. The low order modes show good agreement in terms of both frequency and mode shape correlation, but the fidelity of the results deteriorates rapidly beyond the sixth mode. The first 9 modes from the ANSYS model are shown in Fig. 3. Modes 1 and 2 are the first order bending modes in the lateral and vertical directions, respectively. Mode 5 is the
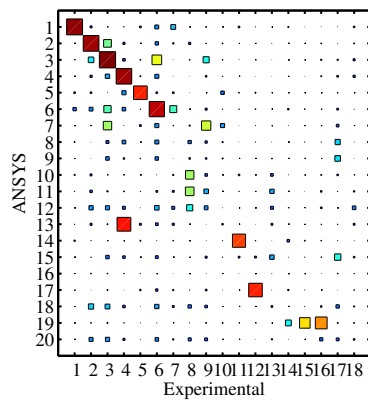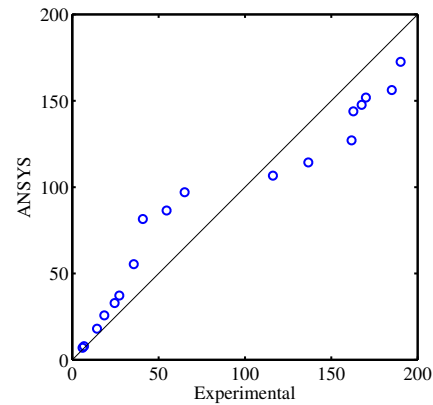
(a) Lynx helicopter.

(b) Tail boom mounted on reaction wall.

Figure 1: Photographs of the Lynx Mk 7 used in preliminary experimental tests.

(a) Modal Assurance Criterion

(b) Frequency correlation (Hz)

Figure 2: Comparison of the experimental modal results for the Lynx tail boom with the ANSYS FE model.

second order bending mode in the vertical plane, and modes 3, 4 and 6 are composed of tailplane flapping and tailboom twisting components.

In the model the axial loading is established through the attachment of a tensioning cable running the length of the tail boom. One end of the wire is attached at the centre of the tail root, with the other attached to a bulkhead toward the aft of the tailboom. The cable is modelled using 10 steel beam elements with a cross sectional area of 0.001m^2 and symmetrical second moments of area of 10^{-9}m^4; the intention being to simulate a sturdy cable with low bending stiffness. The ends of the wire are pinned at the attachment points.

The first buckling mode occurs at 247kN and is shown in Fig. 4. The failure mode is seen to be characterised by local panel buckling in a small locale along one side of the tail boom. To determine the variation of the low order vibration modes under this loading, a sensitivity analysis is carried out using the Gradient Descent method in the ANSYS Design Optimisation tool. For this analysis the tensioning wire is removed from the model and the loads applied directly to the wire attachment points to avoid interference of the cable modes with the primary structure's modes. The results of this study are seen in Table 1 along side the loads required to produce 1% and 2% shifts in each frequency. Up to the first buckling load the first 9 natural frequencies of the tail boom change by less than 1%.

This behaviour is further illustrated in Fig. 5, which shows the first 38 frequency loci (including cable vi-

7.0456Hz · 7.9506Hz · 18.131Hz

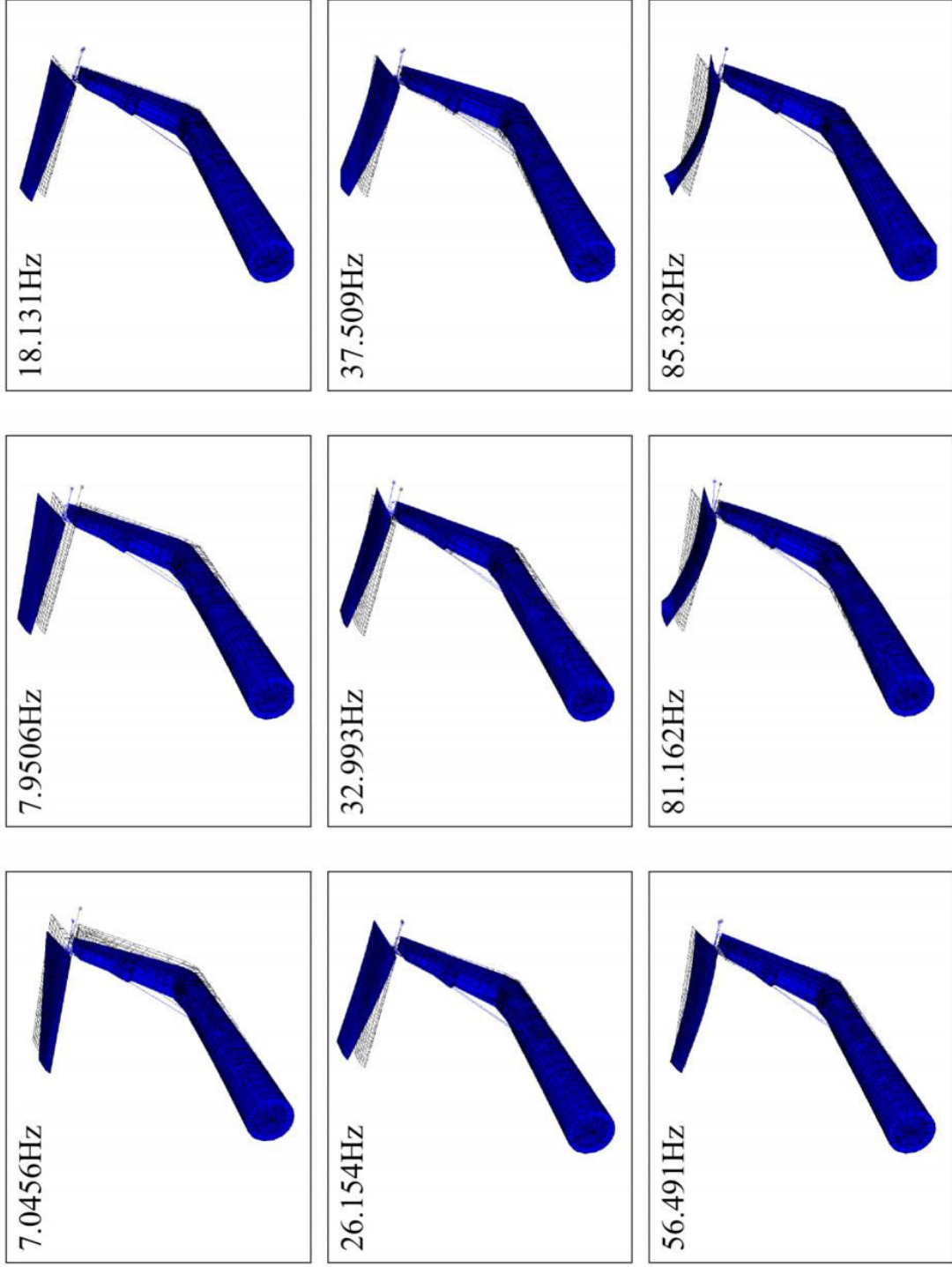26.154Hz · 32.993Hz · 37.509Hz

56.491Hz · 81.162Hz · 85.382Hz

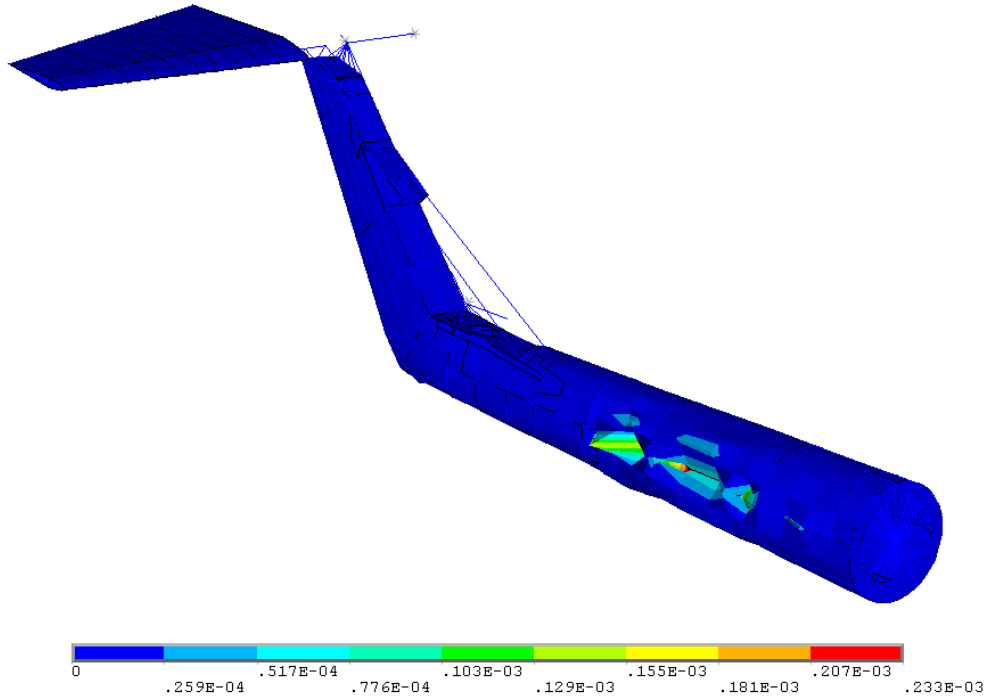Figure 3: Modal results from the ANSYS FE model of the Lynx tail boom.

Figure 4: First buckling mode of the tail boom with the bulkhead reinforced for the tensioning wire attachment.

Mode	Freq.(Hz)	Freq. sens.(HzN^{-1})	1% shift load (N)	2% shift load (N)
1	7.12	-1.16×10^{-7}	-6.19×10^{5}	-1.24×10^{6}
2	7.98	8.67×10^{-8}	9.25×10^{5}	1.86×10^{6}
3	18.22	-5.17×10^{-8}	-3.54×10^{6}	-7.12×10^{6}
4	26.26	-7.53×10^{-8}	-3.51×10^{6}	-7.05×10^{6}
5	33.47	3.33×10^{-9}	1.01×10^{8}	2.03×10^{8}
6	37.80	-2.51×10^{-7}	-1.51×10^{6}	-3.04×10^{6}
7	56.68	-1.46×10^{-8}	-3.92×10^{7}	-7.87×10^{7}
8	81.37	-2.30×10^{-8}	-3.56×10^{7}	-7.16×10^{7}
9	85.40	-1.42×10^{-9}	-6.04×10^{8}	-1.21×10^{9}

Table 1: The frequency sensitivities for the first nine tail boom modes, along with the corresponding loads required to produce 1% and 2% changes in each of the frequencies.
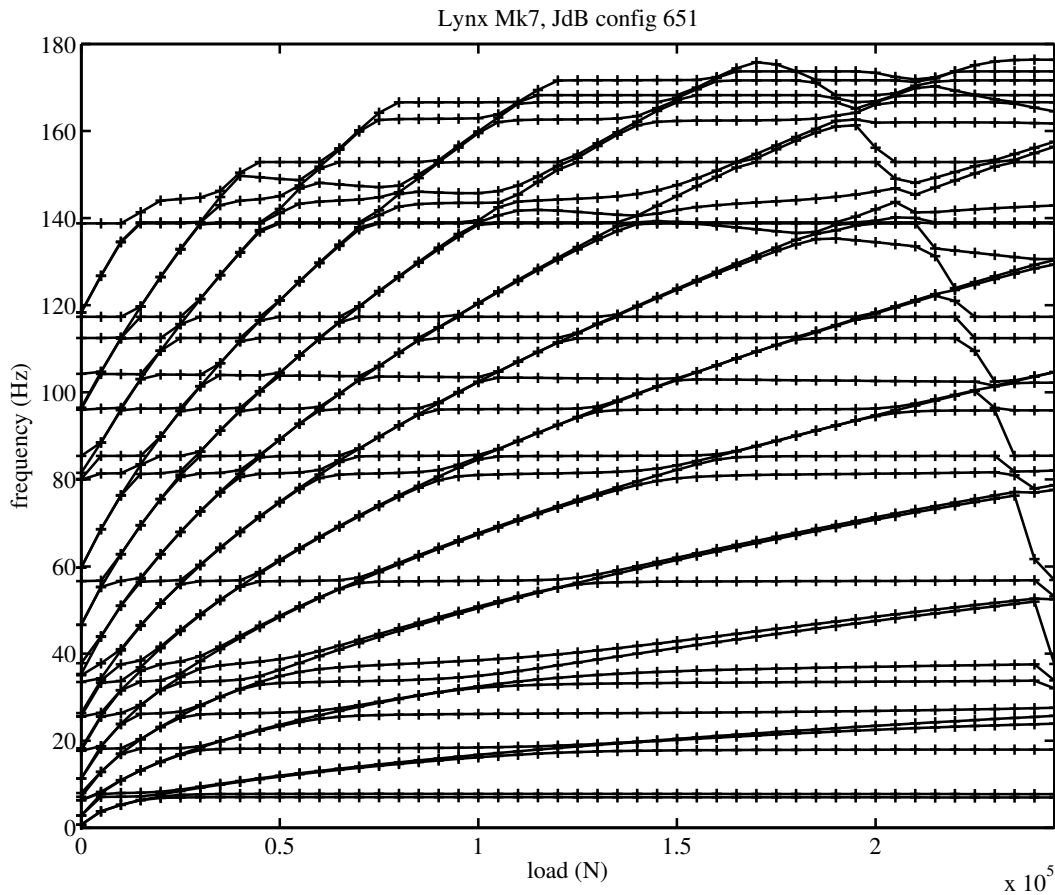
Figure 5: The first 38 frequency loci of the tail boom with the axial tensioning wire, loaded up to the first buckling load. Mode tracing has not been employed in the production of this plot.

bration modes) over a range of loading up to the first buckling load. The tensioning wire modes are seen to rise steeply with increased stress stiffening while the tail boom modes fall almost imperceptibly. As the buckling load is approached, a high order mode shows a rapid decrease in its natural frequency, reaching zero at the buckling load. This corresponds with a reduction in the effective stiffness of that mode. In contrast to a simple beam, which buckles as its first bending mode's stiffness reduces to zero, the tail boom vibration mode associated with the first buckling mode is a high order localised panel vibration corresponding with the localised buckling failure mode.

3 ATVA in Lynx Tail Boom

It has been stated that a TVA has two beneficial effects: firstly, shifting a natural frequency away from an excitation frequency, and secondly, positioning an antiresonance at the the excitation frequency for a critical location on the primary structure. Both of these effects are produced by a manifestation of eigenvalue curve veering [13, 14, 15]. As the TVA is tuned, the eigenvalue of the absorber mode approaches that of the primary structure, but in the vicinity of the 'tuned' condition, the two eigenvalue loci veer away from one another. The natural frequencies can thus be controlled in this manner, and at the point of attachment for the TVA an antiresonance will always be sandwiched between the two eigenvalues and is manipulated along with the natural frequencies.

Fig. 6 shows the behaviour of the eigenfrequencies in an enlarged, higher resolution region of Fig. 5. An ax-

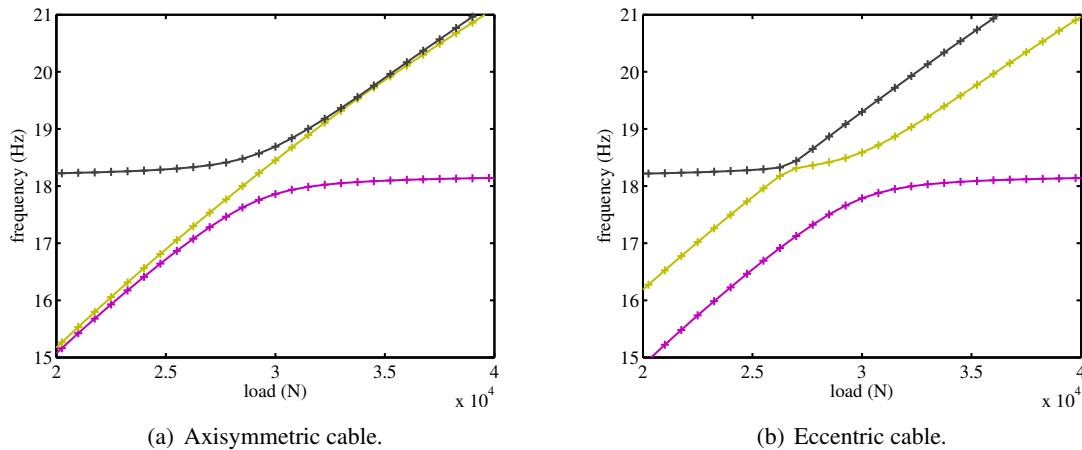(a) Axisymmetric cable. (b) Eccentric cable.

Figure 6: Example of three veering frequency loci, using two different cable profiles.

isymmetric cable has two orthogonal modes at each natural frequency, and these are seen traversing Fig. 6(a) together with positive gradient. In the veering region, however, one of the cable mode frequency loci is seen to veer while the other seems unaffected. To examine this behaviour further, the symmetry of the cable in the model is broken by quintupling the second moment of area in the vertical plane and dividing that in the horizontal plane by five[1] The result in Fig. 6(b) is that the two cable modes become separated, and one is seen to interact very weakly with the primary structure's mode while the other reacts more strongly. The strong modal interaction indicates a large coplanar component of vibration in the two modes. Despite the weak in-plane interaction of the out-of-plane cable mode, concerns arise that it may result in detrimental resonance at 'tuned' condition ($\sim$3N, $\sim$18Hz) of the axisymmetric cable in Fig. 6(a). For this reason, and to distinguish the effects of the modes more clearly, the remaining studies in this section adopt the eccentric cable design of Fig. 6(b).

The natural frequencies for this configuration are computed for 100 load steps in the range 0N to 75kN, representing 30% of the buckling load, and plotted in Fig. 7. Once again the cable modes show increasing frequencies with cable tension while the tail boom modes remain almost constant, except in the regions where the frequency loci intersect. In these regions the effect of frequency veering can be seen to perturb the priamry structure's natural frequencies. A feature of the continuous mass and stiffness distribution in the cable ATVA, in contrast to the discrete, lumped properties of a 1DOF ATVA, is that each of the cable modes can be used as the effective ATVA mode. This has two ramifications: firstly, by using higher order modes to mitigate higher excitation frequencies and response modes, the ATVA can operate over a large frequency range with lower actuation capabilities and the associated reduction in weight and power requirements. Alternatively, a faster response could be obtained for the same actuation performance. The second opportunity that presents itself is the operation of the absorber to mitigate multiple excitation frequencies. This would rely on those excitation frequencies coinciding with the harmonics of the first cable mode, but in the case of rotorcraft vibrations the excitaiton is primarily restricted to the rotor frequency, the blade passing frequency, and multiples thereof, and the potential for the simultaneous mitigation of all these harmonic components is a concept that merits further investigation (but not here).

Frequency response functions (FRFs) are computed in ANSYS for the same configuration. The excitation is applied at a reinforced section mid-way down the tail. The response is measured at the wire attachment point in the aft bulkhead. Figure 8 shows the FRFs for horizontal and vertical excitation and response

---

[1]This alteration is equivalent to flattening the cable into a deep, slender beam. It should be noted that some of the assumptions of the beam element derivation are violated in this embodiment; in particular the described beam will experience high torsional distortions to the point of geometric nonlinearity. This implementational obstacle is overlooked in this context to allow the exploration of the concept.
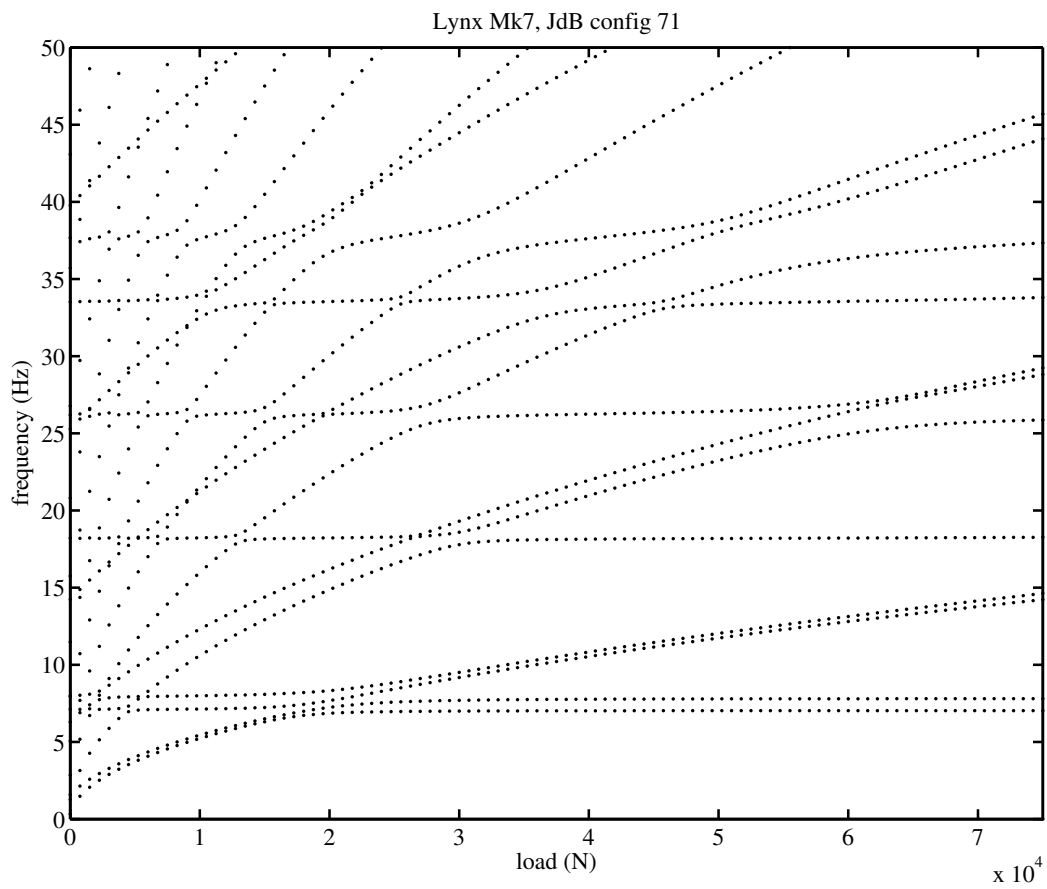
Figure 7: Frequency loci of the tail boom with the *eccentric* TVA cable.

(a) horiz-horiz   (b) horiz-vert
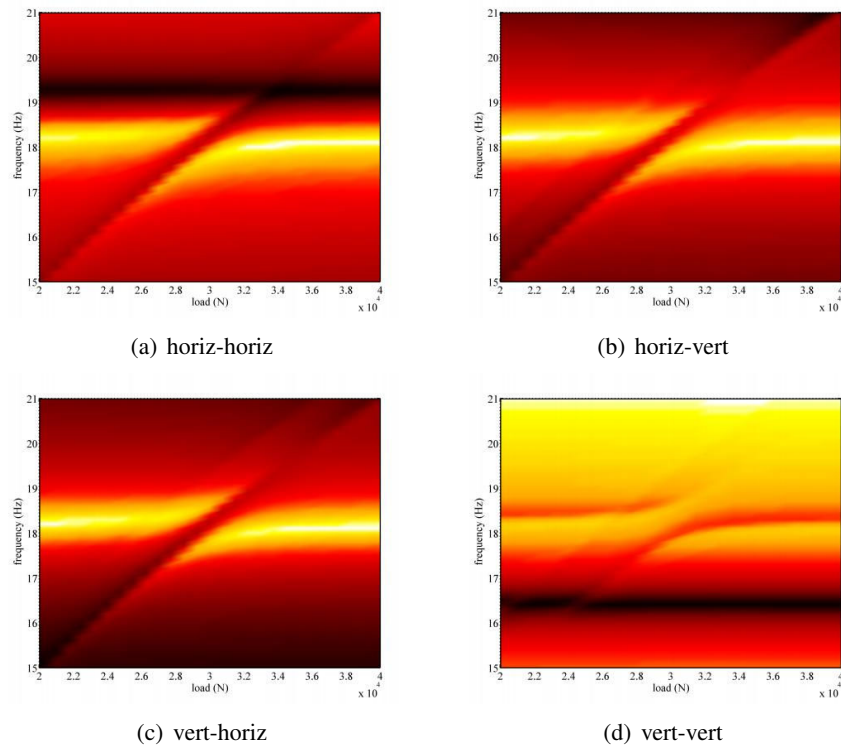
(c) vert-horiz   (d) vert-vert

Figure 8: Response contours for the 18 Hz mode. Light regions denote high response. Captions indicate excitation-response directions.

measurements corresponding to the region examined above in Fig. 6(b). In all four figures the resonant peaks are seen to veer with an antiresonance running up between them. The FRF curves are plotted for two load cases in Fig. 9, and show the characteristic TVA behaviour where a single resonant peak is replaced by two resonant peaks either side. The most interesting feature of these plots, however, is the contribution, or lack thereof, of the out-of-plane cable mode. It can be seen as a faint resonance running close to a faint antiresonance, but their effect is trivial in comparison to the response of the main structure. Similarly, the effect of the veering cable mode is diminished away from the tuned condition. This observation suggests that the primary structure is not adversely affected by resonant cable modes, yet these modes can still be used to manipulate the natural frequencies and antiresonances of the primary structure itself. This should be true even for the case of a symmetric cable, with a cable resonance coinciding with the tuned condition, although it should be noted that resonant response in the cable may be detrimental to the health of the absorber itself.

This section is concluded by examining the FRF contours over a more comprehensive load and frequency range. The behaviour discussed above is seen to be consistently reproduced, to greater or lesser extent, for all instances of intersecting cable and tail boom mode pairs in Fig. 10. The figure highlights instances which could be used to address narrow-band resonant response of each of the first 6 modes, all requiring cable tensions of less than 15% of the first axial buckling load of the tail boom.

4 Experimental Validation

For experimental validation of the cable ATVA concept, a reduced-scale structure was designed to represent the important dynamic characteristics of the tail boom. The geometry of the FE model is seen in Fig. 11(a), and the structure is pictured in Fig. 11(b). It is constructed primarily from 2mm sheet acrylic which means it exhibits higher levels of damping than a metal structure but is easier to fabricate, as well as allowing
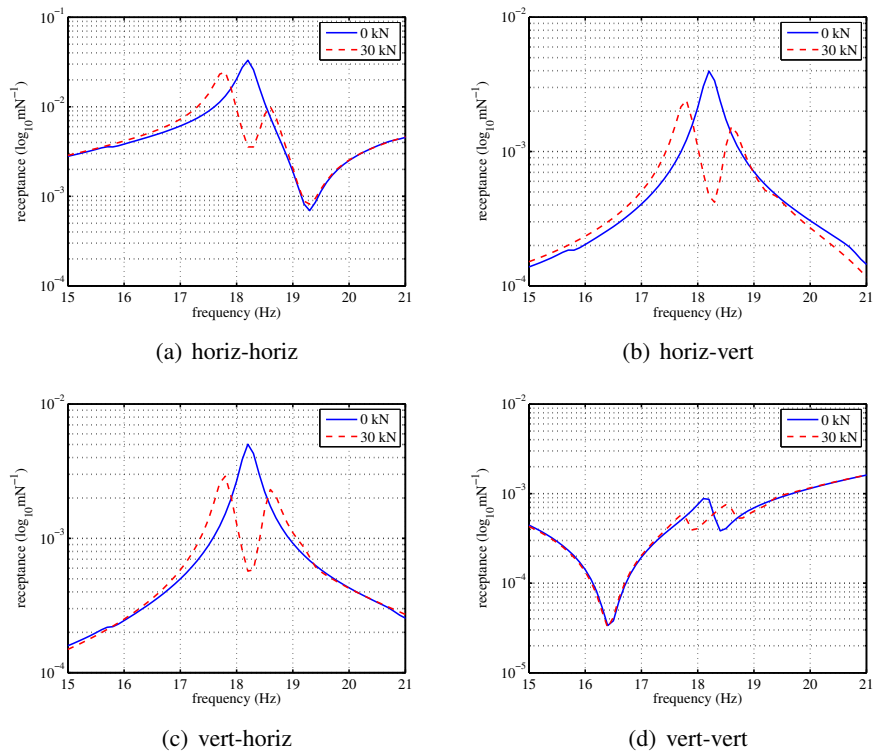
Figure 9: Illustration of the 18 Hz mode's response to the TVA. Captions indicate excitation-response directions.
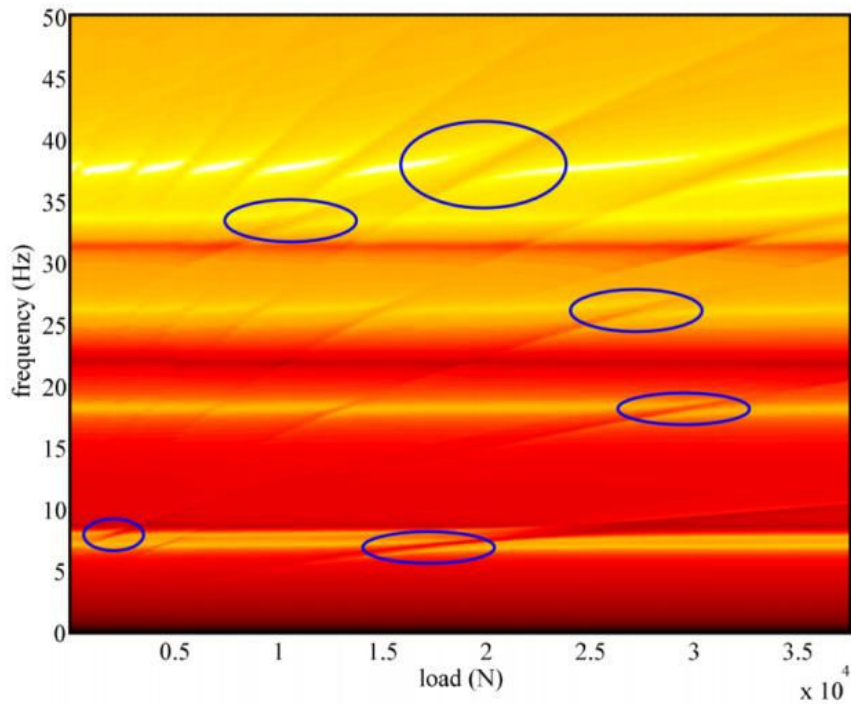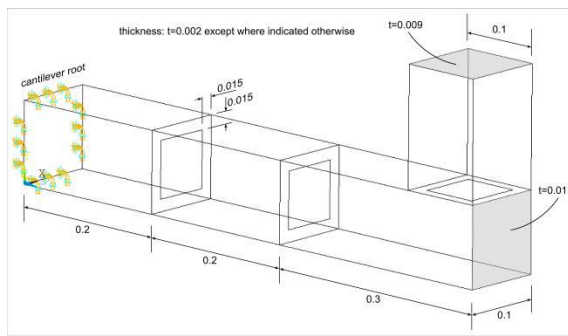

Figure 10: Examples of suitable response regions for TVA implementation. Antiresonances bisect the natural frequencies in the highlighted regions.

(a) FE model geometry

(b) Experimental setup

Figure 11: Reduced-scale representative model of the tail boom

inspection of the internal parts. The Young's modulus is 3.2GPa, the density is 1185kgm^{-3}, and the Poisson's ratio is 0.4. The top section of the tail fin is constructed of thicker material as indicated in the diagram, to add weight and create representative torsional modes in the boom. The hollow box section is stiffened with ribs so that beam-like bending modes are reproduced: without stiffening ribs the full-length side panels flex independently instead of bending together. Finally, the cable is clamped at the free end of the boom using two thicker sheets of acrylic, and these are modelled in the FE model as a single thicker section at the rear as indicated.

The acrylic structure is mounted to a steel support, where the cable passes through a hole and attaches to a turnbuckle. The turnbuckle is used to tension the cable and the load is measured using a load cell comprised of two strain gauges mounted either side of a waisted bolt in line with the turnbuckle. At each load a loose sheet of acrylic is clamped in place to constrain the cable where it passes through the hole at the root of the tail boom, allowing modal tests to be performed. LMS modal testing software is employed for hammer testing, using a least squares complex exponential (LSCE) method to determine the modal properties from the resultant FRFs.

The FE model is meshed using rectangular shell elements with uniform 10mm edges. The first 9 modes from the model are shown in Fig. 12. These modes mirror the behaviour of the full tail boom: the first two modes are the first bending modes in the lateral and vertical directions, respectively; the third mode is a torsional mode; the fourth mode is a tail fin mode, closely related to the tailplane modes of the full Lynx tail boom; the eighth mode is a higher order vertical bending mode; and the remaining modes exhibit localised panel vibrations. The natural frequencies are higher than the Lynx tail boom but share a similar distribution.

The natural frequencies of the FE model are compared to the baseline experimental results in Table 2. The first two natural frequencies are significantly lower in the experimental structure, and this is attributed to high flexibility in the root constraint for these preliminary tests. The remaining modes show reasonable agreement; the torsional mode is unaffected by this flexibility and is well constrained in the experiment, while the higher order and bending modes are affected to a lesser extent. The local panel buckling modes were not picked up in the experiemental tests, as expected due to the small motions of these modes at the free end of the tail boom as seen in Fig. 12.

Initial experiemental results with the cable TVA are shown in Fig. 13. Three FRFs are seen, corresponding with points close to the free end of the tail boom, in the three translational directions. The low order modes are clear and distinct but the higher order modes are heavily influenced by the damping of the acrylic structure. Both figures demonstrate the TVA tuned to the 3rd tail boom mode at 120Hz, with the 2nd cable mode being used in Fig. 13(a) and the 3rd cable mode being used in Fig. 13(b). Both cases produce an antiresonance at the centre of the tail boom mode, but that of the 2nd cable mode is more pronounced, prompting speculation that the higher order cable modes are less effective than the low order modes. Another feature of the results is that the antiresonance spans a low bandwidth, and would require accurate tuning to produce
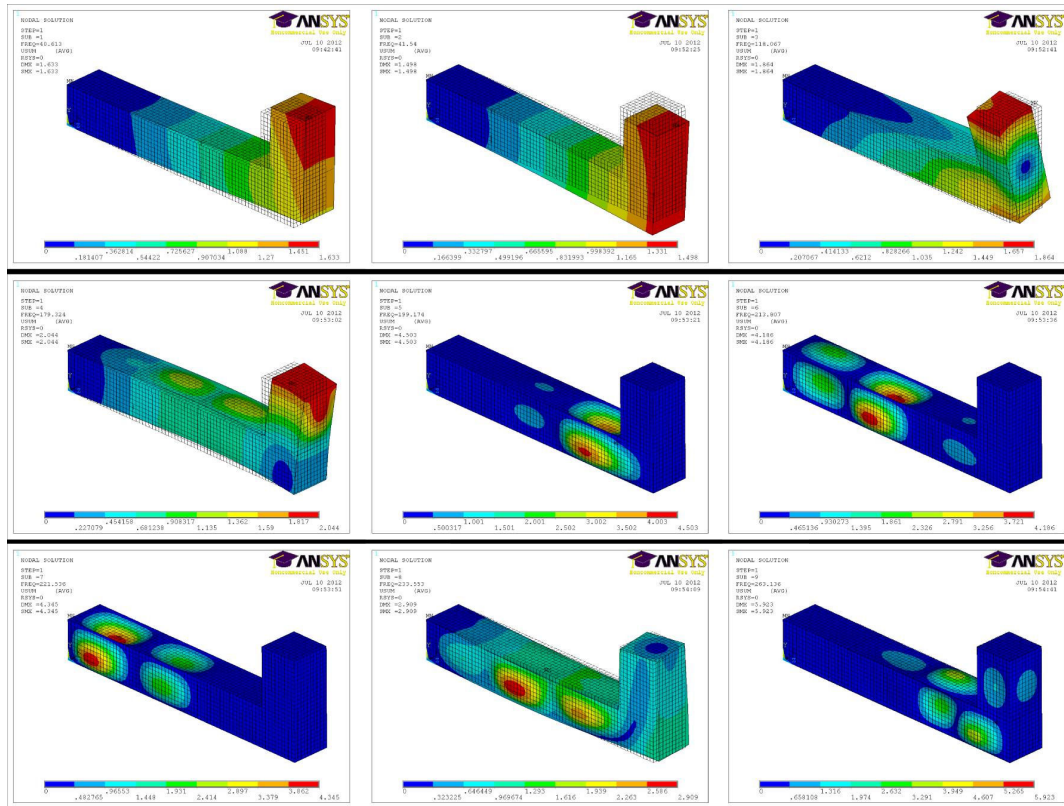
Figure 12: The first 9 modes of the acrylic tail boom model, from the FE model

Mode	FE model (Hz)	Experimental (Hz)	mode type
1	40.6	5.05	1st lateral bending
2	41.5	16.1	1st vertical bending
3	118	120	torsional
4	179	168	tail fin
5	199	–	local panel
6	213	–	local panel
7	222	–	local panel
8	234	223	2nd vertical bending
9	263	–	local panel

Table 2: Comparison of natural frequencies of the acrylic tail boom, experiemntal and analytical.

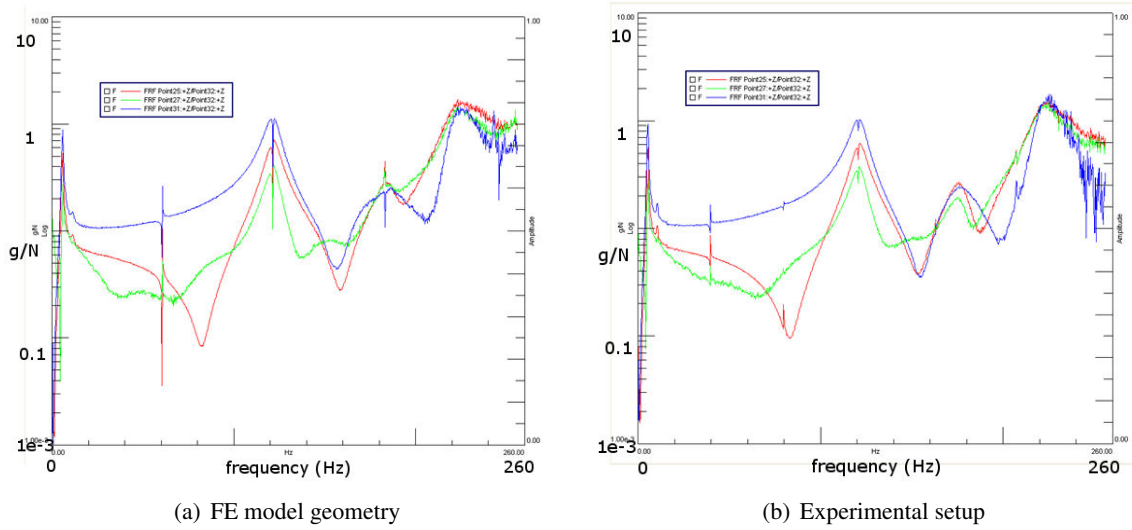(a) FE model geometry   (b) Experimental setup

Figure 13: Reduced-scale representative model of the tail boom

good results. A heavier cable could offer improved coupling to the modes of the primary structure. A final observation is that the 3rd cable mode, at ∼180Hz in Fig. 13(b), appears to cause a spike as opposed to an antiresonance in two of the measured degrees of freedom. It is possible that this reflects the condition discussed with reference to Fig. 6(a) above, where one of the orthogonal modes in an axisymmetric cable does not interact with the primary structure's modes and creates a resonance countering the main antiresonance. The quality of this preliminary data is not very high, however, and further investigations are needed to support such conjectures.

5 Conclusions

A Lynx tail boom model has been validated with respect to the first 6 modes taken from experimental data. This model has then been used to evaluate the performance of a cable-based adaptive tuned vibration absorber for use in this context. The cable is mounted inside the tail boom, running axially along its length, and it is found that tensioning of the cable up to the first buckling mode of the tail boom produces only negligible variation in the low order bending modes of the structure. The cable modes, however, see pronounced variation in frequency over this loading regime, and their interactions with the strucutral modes have been shown to be effective in mitigating vibrations in the same manner as a vibration absorber, for all six tail boom modes studied.

A result of the continuous mass and stiffness distribution in the absorber is that the cable has multiple modes, at harmonics of the first mode, each of which can be used as the tunable absorber frequency. This offers the benefit of increased frequency range with lower actuation requirements, although preliminary exeriments suggest that the higher order cable modes are less effective in this capacity.

A problem arising with symmetric cable profiles is that one of the two orthogonal modes at each cable frequency is often seen to coincide with the excitation frequency in the tuned condition, possibly causing detrimental response in the cable itself, although FE results suggest the effect on the main structure to be minimal. It has been shown that breaking the symmetry of the stiffness, for example through the use of an eccentric profile, can offset the two cable modes' frequencies, thus ameliorating the problem.

A reduced scale experimental model has been presented and preliminary results confirm the findings of the FE studies.

Acknowledgements

References

[1] C.F. Beards. *Structural vibration: analysis and damping*. Butterworth-Heinemann, 1996.

[2] J.P. Den Hartog. *Mechanical vibrations*. Dover Pubns, 1985.

[3] W. Thomson. *Theory of vibration with applications*. Taylor & Francis, 2004.

[4] L. Meirovitch. *Elements of vibration analysis*, volume 2. McGraw-Hill New York, 1986.

[5] W.F. Paul. Vibration damped helicopter rotor, November 1970.

[6] J. Q. Sun, M. R. Jolly, and M. A. Norris. Passive, adaptive and active tuned vibration absorbers—a survey. *Journal of Vibration and Acoustics*, 117(B):234–242, 1995.

[7] L. Kela and P. Vähäoja. Recent studies of adaptive tuned vibration absorbers/neutralizers. *Applied Mechanics Reviews*, 62:060801, 2009.

[8] CE Gough. The theory of string resonances on musical instruments. *Acustica*, 49(2):124–141, 1981.

[9] B. C. Stephens. Natural vibration frequencies of structural members as an indication of end fixity and magnitude of stress. *Journal of the Aeronautical Sciences*, 4:54–56, 1936.

[10] H. Lurie. Effective end restraint of columns by frequency measurements. *Journal of the Acoustical Society of America*, 19:2122, 1951.

[11] J. E. Coote. Consideration of dynamic variability. Technical Report Internal Report, University of Bristol, Bristol BS8 1TR, England, August 2006.

[12] *Release 10.0 Documentation for ANSYS*. Southpointe, 275 Technology Drive, Canonsburg, PA 15317, USA.

[13] Jonathan Luke du Bois. *Adaptive Fuselage Response Suppression*. PhD thesis, University of Bristol, 2009.

[14] J. L. du Bois, S. Adhikari, and N. A. J. Lieven. Eigenvalue curve veering in stressed structures: An experimental study. *Journal of Sound and Vibration*, 322:1117–1124, 2009.

[15] J.L. du Bois, S. Adhikari, and N.A.J. Lieven. On the quantification of eigenvalue curve veering: A veering index. *Journal of applied mechanics*, 78(4), 2011.